SLIDING MODE CONTROLLER OF AUTOMATIC BRAKING SYSTEM

M. A. Subari[1*], K. Hudha[2], N. H. Amer[3]

[1,2,3] Department of Mechanical Engineering, Faculty of Engineering,
Universiti Pertahanan Nasional Malaysia (UPNM), Kem Sungai Besi,
57000, Kuala Lumpur, Malaysia.

ABSTRACT

This paper presents the development of automatic braking system. The brake modeling that consists of brake pedal mechanism, static control valve, air flow dynamic, variable orifice modeling and brake system hydraulic was developed using a MATLAB SIMULINK software. Then, the braking system will be controlled by using a Sliding Mode Controller (SMC) and PID controller. The result obtained will be validated with the brake torque desired for 100 Nm and 50 Nm. of various frequencies. Validation results showed that controller has a better performance compared to the PID controller.

KEYWORDS: *Automatic braking; sliding mode controller; PID controller; particle swarm optimization; desired torque*

1.0 INTRODUCTION

A braking system is needed to halt the vehicle from motion, reduce the vehicle speed as quickly as possible and maintain the vehicle direction stable. The braking system mechanism can be divided into several methods, which are conventional, brake-by-wire, antilock braking system (ABS) and advanced emergency braking system. These methods require a driver so that the braking system can be operating very well. However, with a driver inside a vehicle to stop the motion, it will risk their life and causes injuries during braking and driving (Shaomin, Zhen, Lechao, & Cangsu, 2010).

In order to overcome this problem, an automatic braking system is introduced. This automatic braking will be controlled from a distance. The concept of automatic braking system have been studied in the previously year but unfortunately, the researchers have failed to automatically control the brake smoothly and safely. Several researchers have proposed an automatic braking system for any Intelligent Vehicle and Highway System (IVHS) (Yamada & Sawada, 2001; Fortina & Torino, 2003; Milanés, González, Naranjo, Onieva & De Pedro, 2010) while Maciuca, Gerdes and Hedrick (1993) has indicated the vacuum booster operation as the main part to be

[*]Corresponding Email:muhdakhimullah@yahoo.com.my

controlled. Liang, Chong, No and Yi (2003) proposed a strategy that controls the parameter of diaphragm force and vacuum booster output using a sliding control in order to reduce the brake pressure lag. Choi and Hedrick (1996) used an input delay between control and response to successfully control the brake pressure, but the system has been neglecting the hydraulic dynamic process of braking control. Due to this, a new method was proposed considering the overall braking system including hydraulic dynamics with a sliding control (Gerdes & Hedrick, 1997).

In this paper, a Sliding Mode Controller (SMC) and PID controller is implemented in this braking system to control the force applied on the brake pedal. Performance for both of these controllers will be evaluated and compared where the better controller will be chosen. This will ensure the best performance for the braking system. This paper is organized as follow; next section will describe the development of brake model, which include brake pedal mechanism, static control valve, air flow dynamic, variable orifice modeling and brake system hydraulic. The third section will detail the development of controller using SMC controller and PID controller strategies followed by the final section on result and analysis.

2.0 DEVELOPMENT OF BRAKE MODEL

The operation of braking system is shown in Figure 1, which consists of pedal linkage, vacuum booster and master cylinder (Maciuca & Hedrick, 1995). This brake system is operated by applying a force on the pedal linkage where it transferred to the pushrod before entering the vacuum booster. Within vacuum booster, the pressure will go through from apply chamber into vacuum chamber before passing the diaphragm area. The force generated in diaphragm area will allow the brake fluid to flow under pressure from the master cylinder into the wheel cylinder, which will actuate the brake pad into braking the wheel. In this study, the braking system is to have a single primary master cylinder and brake torque applied into each wheel is assumed to be the same.

Several researchers have studied and developed a brake model that is very complex for the controller development or simulation. Fisher (1970) has developed a complete brake system consist of 18 states such as dynamics of the pedal, vacuum booster, master cylinder and brake lines. Khan and Kulkarni (1994) have updated the brake system modeling with only 10 states and evaluated the system for slow brake applications. However, the model developed has neglected the important parts in braking system such as master cylinder seal friction and reaction washer hysteresis. A five-state braking system modeling has been introduced with vacuum booster hysteresis and brakes hydraulic are not fully covered (Gerdes, Maciuca, Devlin, & Hedrick 1993). In this paper, a reduced order model of braking system that consists of only four states will be developed based upon the dynamics of air flows and static force balance.

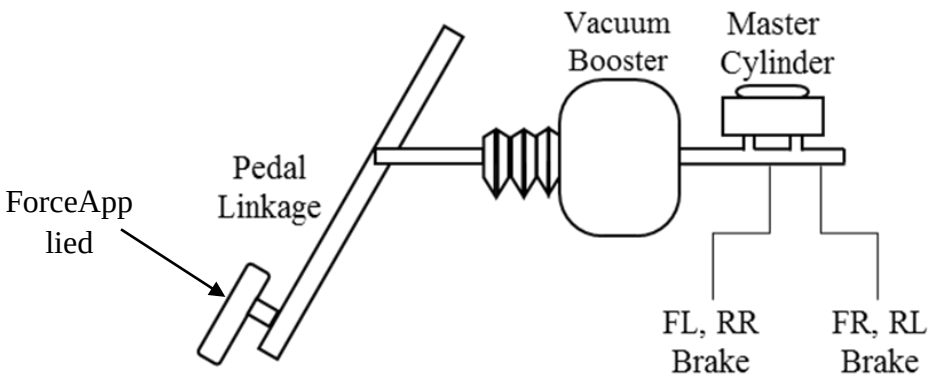

Figure 1. Brake system components

2.1 Brake Pedal Mechanism

Figure 2 shows free body diagram of a pedal linkage normally used in a vehicle (Aparow, Ahmad, Hassan & Hudha, 2012). The pedal linkage consists of two members connected to each other. The pedal force is applied on Member 1. Then, the force is transferred to vacuum booster through push rod by a Member 2 that is pivoted to Member 1. The applied force (0% to 100%) controls the pressure in the vacuum booster (Krishnamachari, 1996). The equation of the brake pedal mechanism is described as below.

$$\sum M_{pivot} = 0 \tag{1}$$

$$\left(F_{in}\cos\phi\right)\left(x_2\cos\theta\right) = \left(F_{pedal}\cos\theta\right)\left(x_0\cos\theta\right) \tag{2}$$

$$F_{in} = \frac{\left(F_{pedal}\cos\theta\right)\left(x_0\right)}{\left(x_2\cos\phi\right)} \tag{3}$$

where

Θ = angle of member 1

Φ = angle of member 2

F_{pedal} = force from human input

F_{in} = input force to vacuum booster

X_0 = total distance from pivot 1 to brake pedal

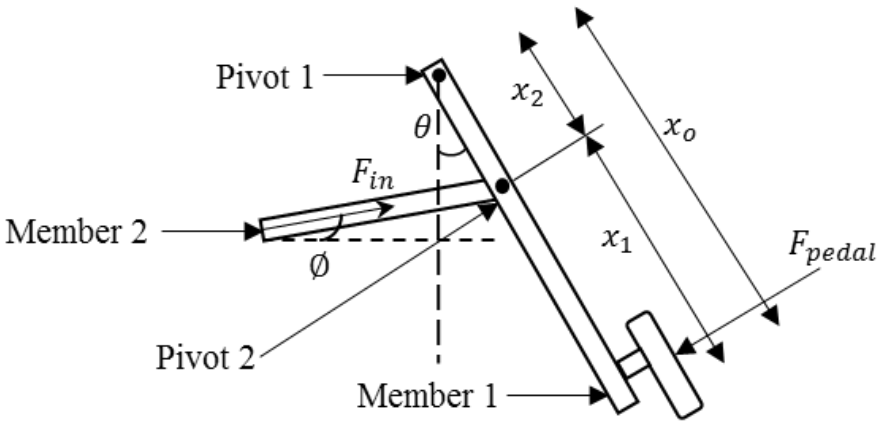

Figure 2. Brake pedal linkage

2.2 Static Control Valve Model

Figure 3 shows the vacuum booster construction with the addition of pushrod and power piston (Gerdes & Hedrick, 1997). The individual force balance for the pushrod and power piston can be described as:

$$F_{in} - F_{vs} - F_{pr} = m_{pr}\ddot{x}_{pr} \tag{4}$$

$$F_d - F_{rs} + F_{vs} - F_{pp} = m_{pp}\ddot{x}_{pp} \tag{5}$$

F_{vs} and F_{rs} represent the force in the valve spring and return spring, m_{pr} and m_{pp} denote the masses of the pushrod and power piston while x_{pp} and x_{pr} are the displacements of power piston and pushrod from the rest state. By assuming the diaphragm area, A_d in apply chamber and vacuum chamber are the same, the diaphragm force F_d is given by:

$$F_d = A_d\left(P_a - P_v\right) \tag{6}$$

where

P_a = pressure in apply chamber

P_v = pressure in vacuum chamber

$$F_{pr} + F_{pp} = F_{out} \tag{7}$$

F_{pr} and F_{pp} represent the force fed back through the reaction washer to the pushrod and power piston while F_{out} denotes the output force from the vacuum booster. Equation (4) to (7) form the basis of a four-state control valve model. The relative displacement of the pushrod and power piston (x_{pr} - x_{pp}) can be used to determine the stage of operation (apply, hold or release).

However, force produced due to the inertial effect of pushrod and power piston motion in the booster is significantly small. By neglecting inertia, Equation (4) to (7) can be simplified into:

$$F_{in} - F_{vs} - F_{pr} = 0 \tag{8}$$

$$F_d - F_{rs} + F_{vs} - F_{pp} = 0 \tag{9}$$

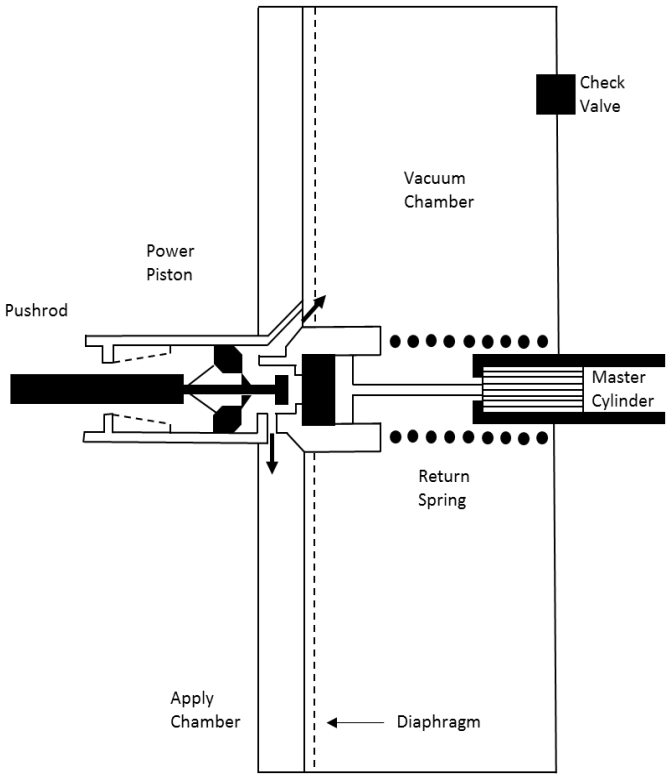

Figure 3. Vacuum booster operation

The overall force balance equation can be obtained by summing the Equation (8) and (9) :

$$F_{out} = \begin{cases} F_d + F_{in} - F_{rs} & F_d + F_{in} \rangle F_{rs} \\ 0 & \text{otherwise} \end{cases} \quad (10)$$

The terms F_{rs} in Equation (10) can be described as

$$F_{rs} = F_{rso} + K_{rs} x_{pp} \quad (11)$$

where

F_{rso} = return spring preload
k_{rs} = spring constant

In order to determine the stage of booster operation, the most straightforward approach is used where F_{pr} and F_{pp} is a fixed percentage of F_{out}. Thus, the stage is given by:

$F_{in} < F_{rel}$ => release
$F_{rel} \leq F_{in} \geq F_{app}$ => hold
$F_{app} < F_{in}$ => apply

2.3 Air Flow Dynamic

Due to the static control valve model, the air that flow through apply and vacuum chamber will determine the dynamic response of the booster. During an application, air flows into apply chamber. This will cause the pressure to increase and forcing the diaphragm forward. Then, the air in vacuum chamber will be compressed and hence the pressure inside vacuum chamber will be increased.

Several researchers have studied various thermodynamic balance of the booster chamber such as Fisher (1970) that assumed adiabatic condition for the booster. Then Khan et al. (1994) also studied adiabatic and isothermal condition for the booster. In this paper, the air masses in the apply and vacuum chamber, m_a and m_v are chosen as the state and by assuming ideal gas behavior and isothermal expansion, the pressure in apply chamber, P_a and vacuum chamber, P_v are:

$$P_a = \frac{m_a RT}{V_{ao} + A_d x_{pp}} \quad (12)$$

$$P_v = \frac{m_v RT}{V_{vo} - A_d x_{pp}} \tag{13}$$

where R is the gas constant, T is the air temperature, V_{ao} and V_{vo} are the initial volumes in apply and vacuum chambers respectively. The state equation then will depend on the stage of operations as follows:

$$\dot{m}_a = \begin{cases} C_{aa}\left(P_{atm} - P_a\right) & apply \\ C_{leak}\left(P_v - P_a\right) & hold \\ C_{av}\left(P_v - P_a\right) & release \end{cases} \tag{14}$$

where

C_{aa} = linearized air flow coefficient for flow from the atmosphere to apply chamber

C_{leak} = linearized air flow coefficient for flow between apply to vacuum chamber

C_{av} = linearized air flow coefficient for flow from vacuum chamber to master cylinder

Then, the mathematical equation for the vacuum chamber is:

$$\dot{m}_v = \begin{cases} \dot{m}_{vm} & apply \\ \dot{m}_{vm} + C_{leak}\left(P_a - P_v\right) & hold \\ \dot{m}_{vm} + C_{av}\left(P_a - P_v\right) & release \end{cases} \tag{15}$$

where $\dot{m}_{vm}$ is the air mass flow rate through check valve. At this valve, the air will flow from vacuum chamber into manifold and hence it can be calculated as:

$$\dot{m}_{vm} = \begin{cases} -C_{vm}\left(P_v - P_{man} - P_o\right) & P_v > P_{man} + P_o \\ 0 & otherwise \end{cases} \tag{16}$$

With P_o is the pressure offset required to open the check valve, P_{man} is the manifold pressure and C_{vm} represents the linearized flow coefficient.

2.4 Variable Orifice Modeling

The size of the valve orifices can be determined from the displacement between the pushrod and power piston. For the fully opened orifice, the flow coefficient C_{aa}, C_{leak} and C_{av} can be determined as follow:

$$C_{aa} = \begin{cases} \overline{C}_{aa} & F_{in} \rangle F_{app} + \overline{F}_{app} \\ \overline{C}_{aa}\left(\dfrac{F_{in} - F_{app}}{\overline{F}_{app}}\right) & otherwise \end{cases} \tag{17}$$

$$C_{leak} = \overline{C}_{leak}\left(\frac{F_{app} - F_{in}}{F_{app} - F_{rel}}\right) \tag{18}$$

$$C_{av} = \begin{cases} \overline{C}_{av} + \overline{C}_{leak} & F_{in} \langle F_{rel} - \overline{F}_{rel} \\ \overline{C}_{av}\left(\dfrac{F_{rel} - F_{in}}{\overline{F}_{rel}}\right) + \overline{C}_{leak} & otherwise \end{cases} \tag{19}$$

where $\overline{C}_{aa}$, $\overline{C}_{leak}$ and $\overline{C}_{av}$ are the initial values of linearized air flow coefficients for flow from atmosphere to apply chamber; flow between apply and vacuum chamber; and flow from vacuum chamber to master cylinder, respectively.

2.5 Brake System Hydraulic

One of the important factors during braking is the brake hydraulic system. It transfer the applied forcefrom human into braking the vehicle. During that process, the hydraulic brake fluid will flow into two circuit for safety precaution where if one circuit malfunction, there is another circuit for braking. Therefore, two master cylindersare needed for this braking hydraulic system. By neglecting the inertia at the piston, the pressure in the primary master cylinder, P_{mcp} can be calculated as:

$$P_{mcp} = \frac{(F_{out} - F_{csp} - F_{cfp})}{A_{mc}} \tag{20}$$

where

F_{csp} = return spring force for cylinder

F_{cfp} = seal friction force for cylinder

The value of F_{csp} can be obtained from return spring preload, F_{cspo} and the coefficient of the return spring, K_{csp} described in equation below:

$$F_{csp} = F_{cspo} + K_{csp}\left(x_{mcp} - x_{mcs}\right) \tag{21}$$

Here, x_{mcp} and x_{mcs} can be denoted as the displacement of primary and secondary piston of master cylinder. Since this research only focusing on single piston of master cylinder, hence x_{mcs} can be neglected.

2.6 Brake and Pads

In the modeling of automatic braking, the most important aspect that need to be observed is the braking torque which is:

$$T_b = K_b P_w V_{mc} \tag{22}$$

Torque obtained from the disc brake assumed to have some friction loses, wrapping in the brake rotor and uneven wear, which are contained within the constant K_b. The empirical data has shown that constant $K_b \leq 0.9$ (Yi et. al. 2001). Meanwhile, P_w and V_{mc} are the wheel pressure and volume of master cylinder respectively.

The volume of master cylinder in Equation (22) can be defined as:

$$V_{mc} = \int \sigma_{mc} C_{mc} \sqrt{\left|P_{mc} - P_w\right|} dt \tag{23}$$

where

$$\sigma_{mc} = \operatorname{sgn}\left(P_{pa} - P_{wa}\right) \tag{24}$$

and

C_{mc} = flow coefficients for brake line

P_{mc} = pressure of master cylinder

P_w = wheel pressure

Figure 4 shows a completed mathematical modeling of the automatic braking system. The system is simulated within MATLAB/SIMULINK while Table 1 lists the parameters for the brake system.

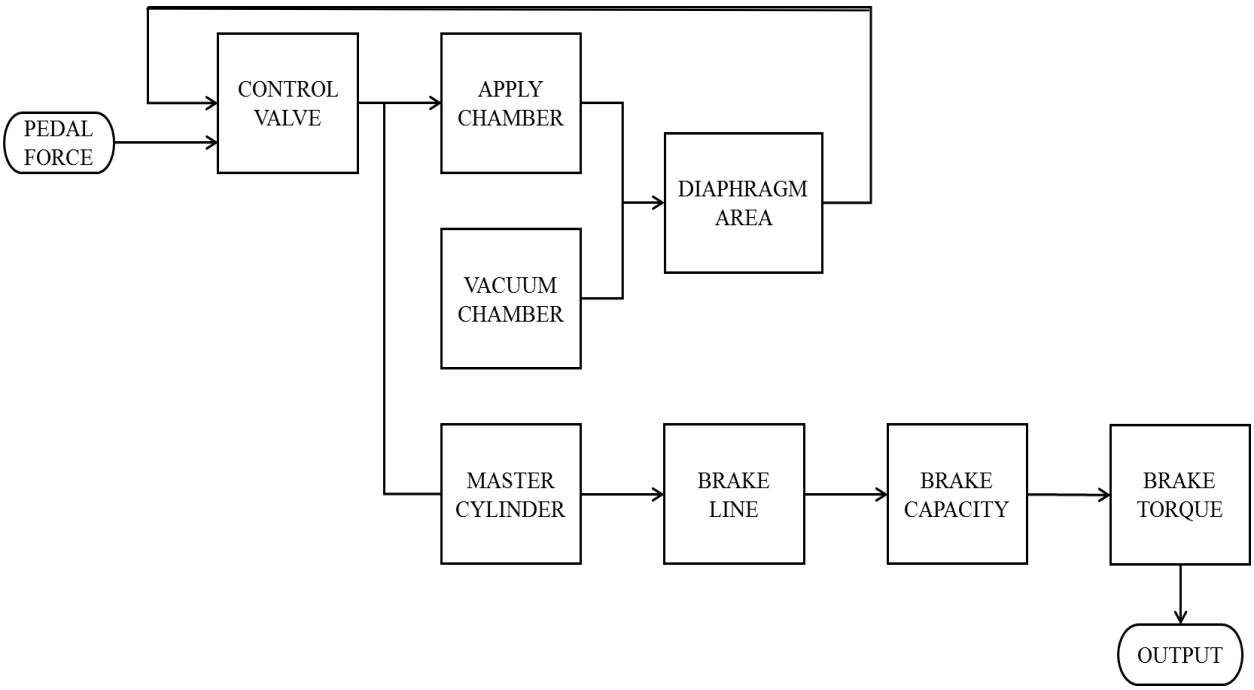

Figure 4. Braking system block diagram

Table 1. Parameter used for the brake system

Symbol	Value
A_{mc}	$4.91 \times 10^{-4} m^2$
A_d	$5.33 \times 10^{-2} m^2$
C_{aa}	$5.8 \times 10^{-5} ms$
C_{av}	$2.2 \times 10^{-4} ms$
C_{qp}	$1.4 \times 10^{-6} kPams^{-1}$
C_{vm}	$1.26 \times 10^{-4} ms$
C_{leak}	$1.4 \times 10^{-7} ms$
F_{rso}	97N
F_{cspo}	90N
F_{cf}	80N
$\overline{F}_{app}$	50N
$\overline{F}_{rel}$	50N
K_{rs}	2411
K_{csp}	2000
K_{bp}	13.333
P_{atm}	101kPa
P_{man}	3000Pa
P_o	10670Pa
T	300K
V_{ao}	$4.3 \times 10^{-4} m^3$
V_{vo}	$2.4 \times 10^{-3} m^3$

3.0 CONTROLLER DESIGN

In this research, two types of controllers have been implemented on the braking system, which is PID controller and SMC controller. For the PID controller, the torque desired is set up by using a positive sign. The maximum torque desired is set at the value of 100 N/m^2. Then the value of KP, KI and KD are tuned manually so that the outputs of the system achieve the torque desired.

While for SMC controller as shown in Figure 5, a control input design used are:

$$u = -U_{saturated}(\dot{\sigma}, \varepsilon) \tag{25}$$

$$u = -U \frac{\sigma}{|\sigma| + \varepsilon} \tag{26}$$

where U is the control input to make the system becomes more stable, and ε is the error rate which must be greater than 0. Guo, Yuzheng and Peng-Yung Woo (2003) described σ as the sliding surface design and can be defined as:

$$\sigma = Ce \tag{27}$$

where

C = constant value
e = input of torque desired

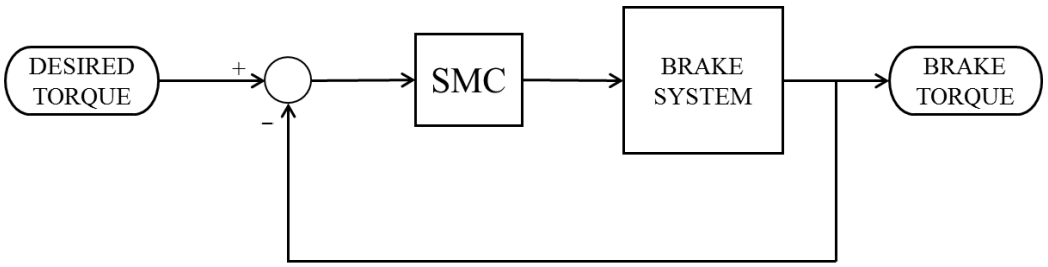

Figure 5. SMC controller of the brake system

4.0 CONTROLLER OPTIMIZATION

The SMC controller was optimized by using a Particle Swarm Optimization (PSO) which first had been introduced in 1995 by Dr. Kennedy and Dr. Eberhart (Yan, Deng, Zhou & Chi, 2012). Due to its simple operation and algorithm, the PSO was chosen as the controller parameters optimization. In the PSO, there are various agents containing a fitness level that moving in swarm. The function of the fitness level is to determine its next position and velocity of travel where the particle with best fitness will be chosen as the solution for the optimization problem. Particle that form at the beginning of PSO process will continue optimized until either algorithm achieve desired result or acceptable solution cannot be found within computational limit. The movement of particle was affected by two factors, which is global particle to best particle solution and local particle iteration-to-iteration best solution.

Position for each particle X_i in PSO can be defined as

$$X_i = \left(X_{i1}, X_{i2}, ..., X_{iD}\right) \tag{28}$$

where

i_{th} = particle number which corresponds to the number of parameters defining the solution

The memory of the previous best solution can be described as

$$p_i = (p_{i1}, p_{i2}, ..., p_{iD}) \tag{29}$$

For each particle number, velocity v_i in each dimension is independently described as

$$v_i = (v_{i1}, v_{i2}, ..., v_{iD}) \tag{30}$$

The velocity is updated after every iteration and the particle will move in randomly to find its own best position, p_{best}, and the global best position, g_{best}. Hence, the Equation (30) will be updated and become:

$$v_{id}^{(t+1)} = w \times v_{id}^{(t)} + c \times U[0,1] \times \left(p_{id}^{(t)} - X_{id}^{(t)}\right) + s \times U[0,1] \times \left(p_{gd}^{(t)} - X_{id}^{(t)}\right) \tag{31}$$

Since the velocity is updated on Equation (31), hence the new position can be determined as:

$$X_{id}^{(t+1)} = X_{id}^{(t)} + v_{id}^{(t)} \tag{32}$$

where

C = weights trading off the impact of the local best solutions
U[0,1] = samples a uniform random distribution from 0 to 1
t = relative time index
s = weights trading off the impact of the global best solutions
w = weight of inertia impact for each particle

The purpose of introducing the PSO in this study is to optimize the values of SMC, which are *U*, *C* and ε as shown in Figure 6. This will cause the swarm particle to have a 3D each and act as an input variables. These values will be applied on the SMC controller model to obtain the optimum brake torque. Hence, it will be an objective function for the optimization problems follow:

Fitness function, $J(X_i) = \sqrt{T_b}$ (33)

where T_b is the brake torque. The personal best record and global best record will be compared with the particle best fitness. Then, position for the best particle will be saved for next iterations. Table 2 shows the parameters use in PSO optimization.

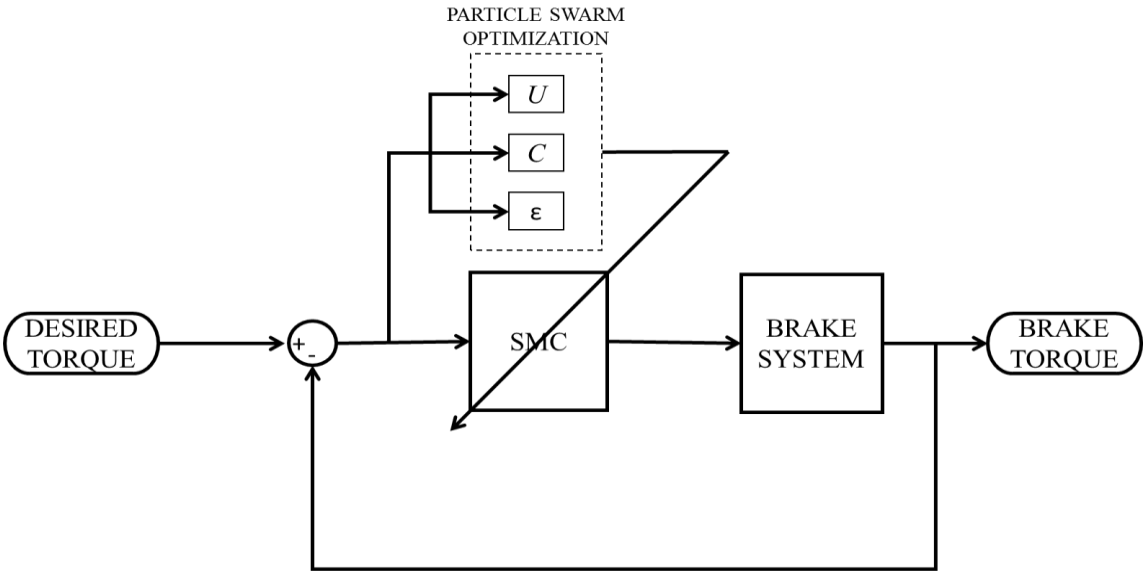

Figure 6. PSO optimization on SMC controller of the brake system

Table 2. Parameter used for PSO optimization

PSO Parameter	Value
d	3
X_i	3
k	10
c	1.42
w	0.9
s	1.42

5.0 RESULTS

In order to evaluate the performance of the brake system model, a series of tests were conducted using different desired brake torque and different frequency. Figure 7 shows the graph of comparison for brake torque by using a SMC and PID controller. The desired brake torque was set at maximum point of 100 Nm with a positive sine wave since the negative pedal force, F_{pedal} does not exist. For the SMC, the value of U, ε and σ were set at 60.1, -0.15 and 59 respectively. Meanwhile the value for K_P, K_I and K_D are 4, 1 and 0. The SMC result seems to follow the desired brake while the PID result was delayed at 0.2 second.

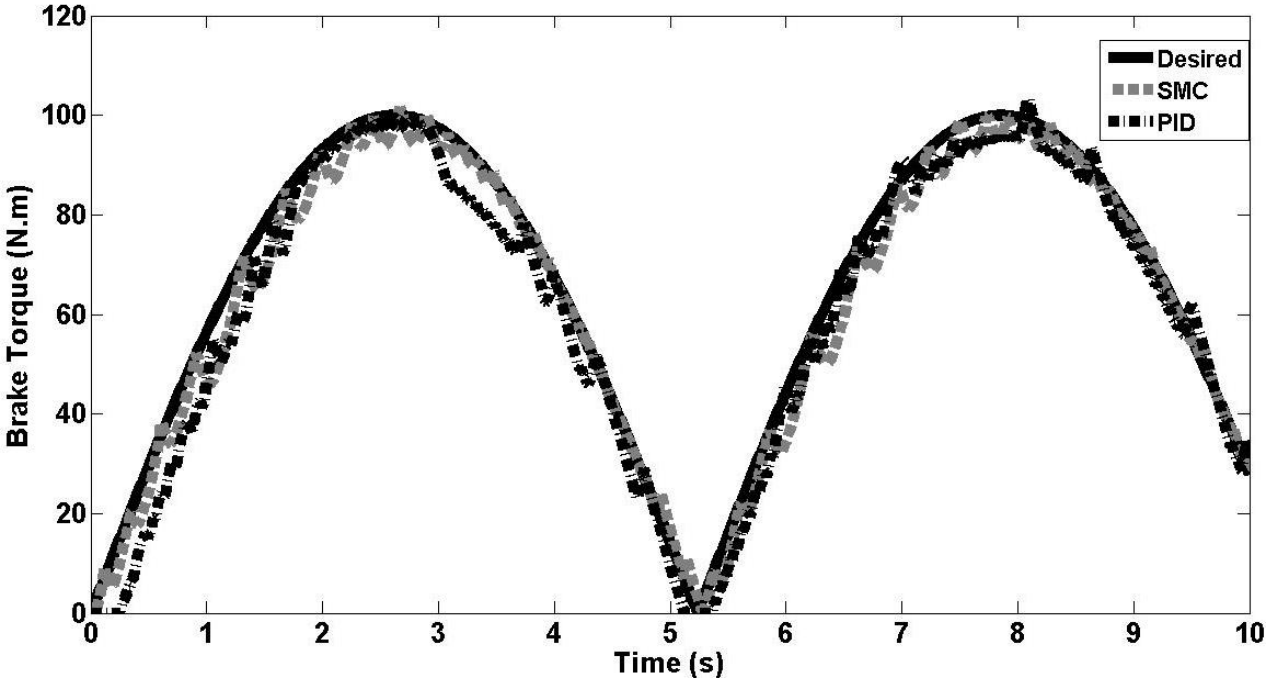

Figure 7. Graph of SMC and PID controller for 100 Nm at 0.5 Hz

Another test was carried out using different set of desired torque. Here, it is set to have maximum of 50 Nm desired torque and the results for both controllers are shown in Figure 8. Similarly, SMC performed better in producing desired braking torque. Meanwhile, PID controller has delayed response of 0.3 seconds and failed to generate the desired braking torque within the first three seconds with maximum torque of 42 Nm only.

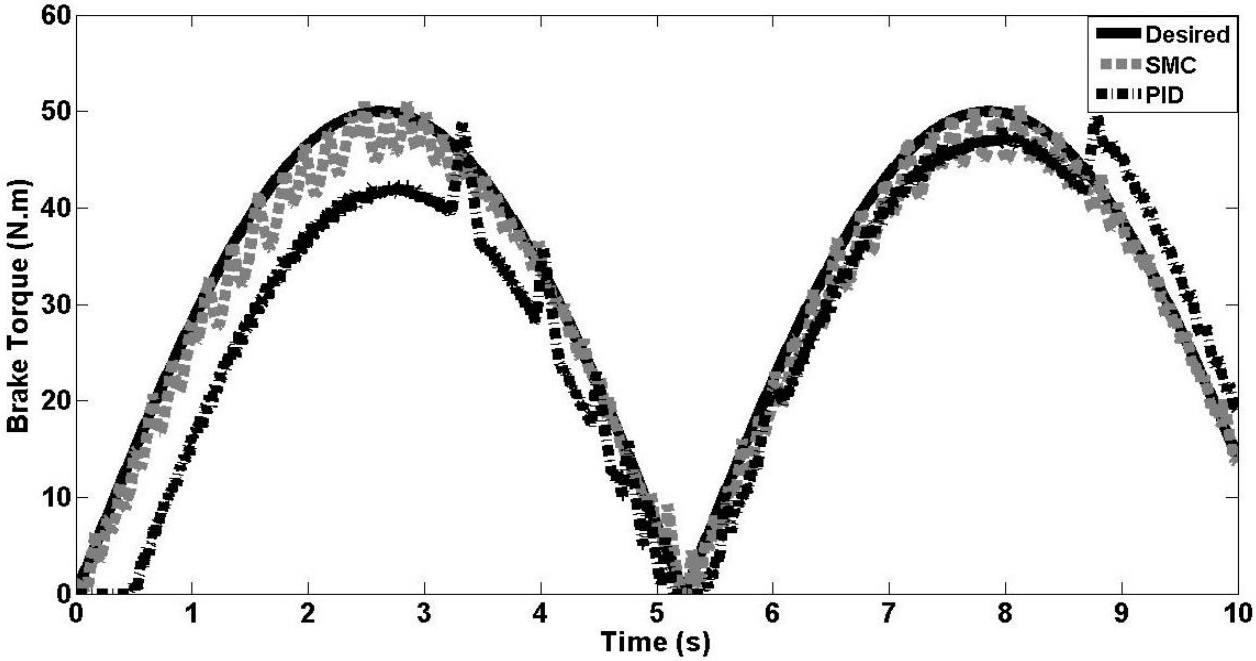

Figure 8. Graph of SMC and PID controller for 50 Nm at 0.5 Hz

Further analysis was carried out where the percentage error within the system was evaluated and compared between system with SMC and system with PID as shown in Figure 9. For PID, the highest percentage error was recorded at 9% while for the SMC the error was 2%. Within a simulation time of 10 seconds, it can be concluded that SMC has the better performance and lower percentage error between 0% to 2% compared to PID within range of percentage error is around 0% to 9%. The graph in Figure 9 also shows that the percentage error for SMC is in overall, better than PID within the 10 seconds simulation time. For the desired brake torque of 50 Nm, the highest percentage error of PID was recorded at 8% compared to SMC, which is 1.5%. Then, error of SMC was compact during a simulation time where it is around 2%. Hence, it can be concluded that SMC has the better performance than PID.

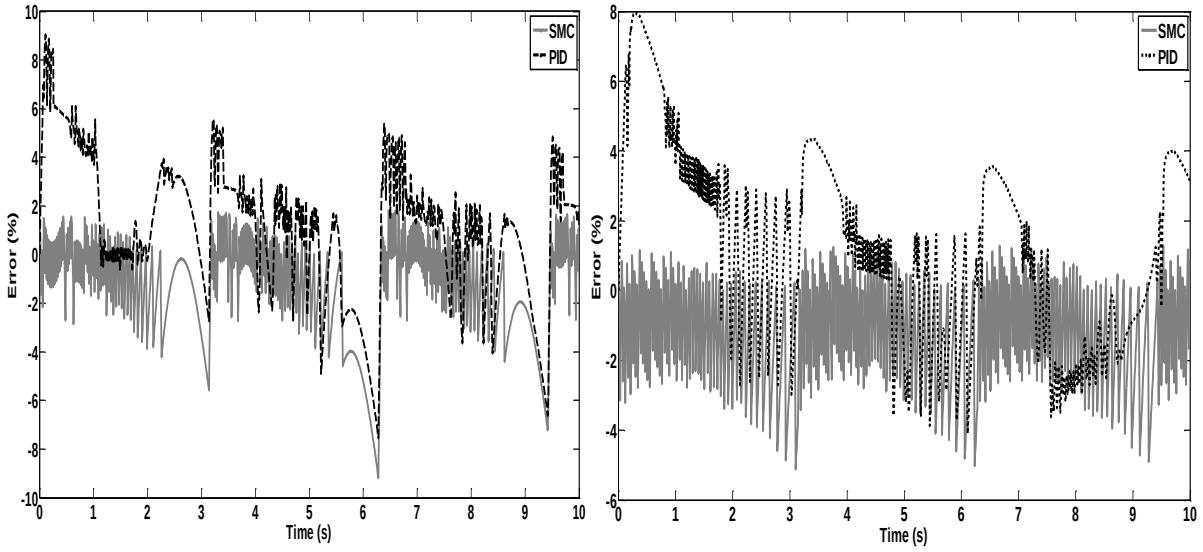

Figure 9. Percentage error of desired brake torque

A further test for brake torque was carried out at different frequency of 0.9 Hz, instead of 0.5 Hz before. Figure 10 shows the brake torque response for 100 Nm sine input. At the starting of simulation, the PID result was delayed while the SMC followed the desired input. The brake torque is released after achieve the desired of 100 Nm, however the SMC and PID does not followed. This is because it is impossible in reality to achieve 0 Nm from 100 Nm in one second. Then, between SMC and PID, it can be said that SMC has a better maximum desired torque while PID has a better minimum torque desired.

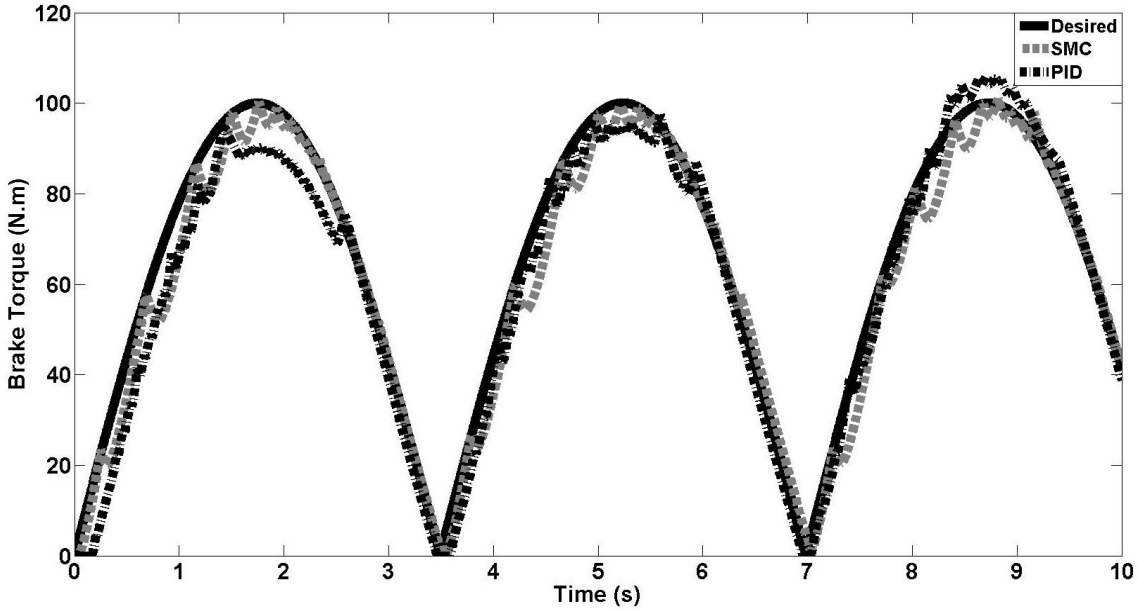

Figure 10. Graph of SMC and PID controller for 100 Nm at 0.9 Hz

Figure 11 shows the simulation result of the brake system for 0.9 Hz with desired brake torque of 50 Nm. The PID result was delayed compared to the SMC and desired brake torque where the SMC has been successful to approach the desired value compared to the Figure 10, both the controller used allows the brake torque to reach 0 Nm easily. This is due to the shortest maximum value of 50 Nm of the desired brake torque.

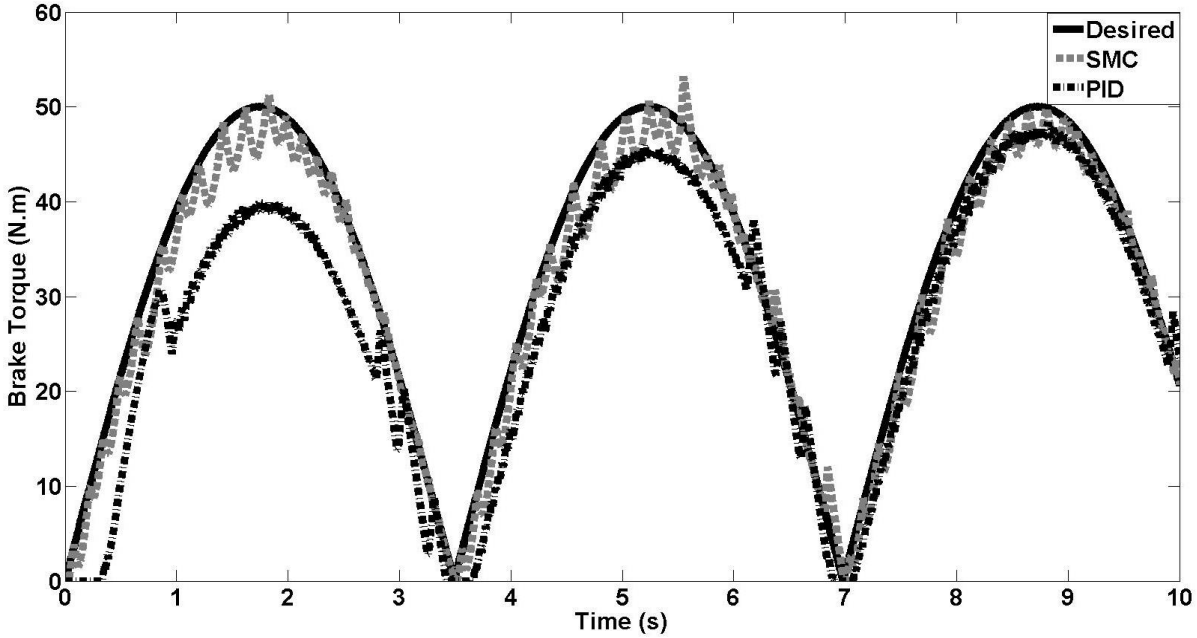

Figure 11. Graph of SMC and PID controller for 50 Nm at 0.9 Hz

Figure 12 shows the 4% error for 100 Nm desired input at 0.9 Hz from Figure 10. The PID controller has the largest percentage error of 9% compared to SMC, 1.5%. Thus, it can be concluded that the SMC has a better performance compared to the PID. Figure 13 shows the percentage error of 50 Nm desired brake torque at 1.5 Hz. The SMC controller has a smallest percentage error of 2% compared to the PID controller of 9%. Hence, it shows those SMC controllers are better controller to be used in the brake system simulation compared to the PID controller.

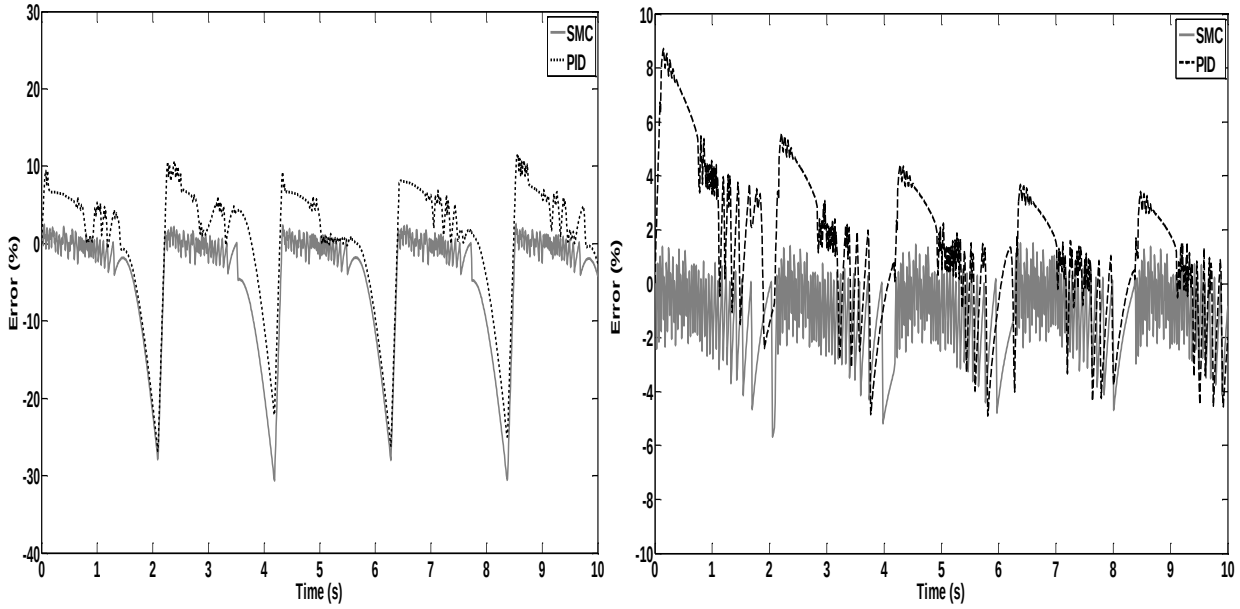

Figure 12. Percentage error of 100 Nm at 0.9 Hz

Since SMC has a better result compared to the PID, a further test was carried out for the SMC to optimize the controller by using a PSO. The result in Figure 13 shows the graph of SMC optimized by PSO for 100 Nm at 0.5 Hz. It show that the optimization result have a better performance compared to SMC. Besides that, it also has a lower percentage error, which is around 0.9%.

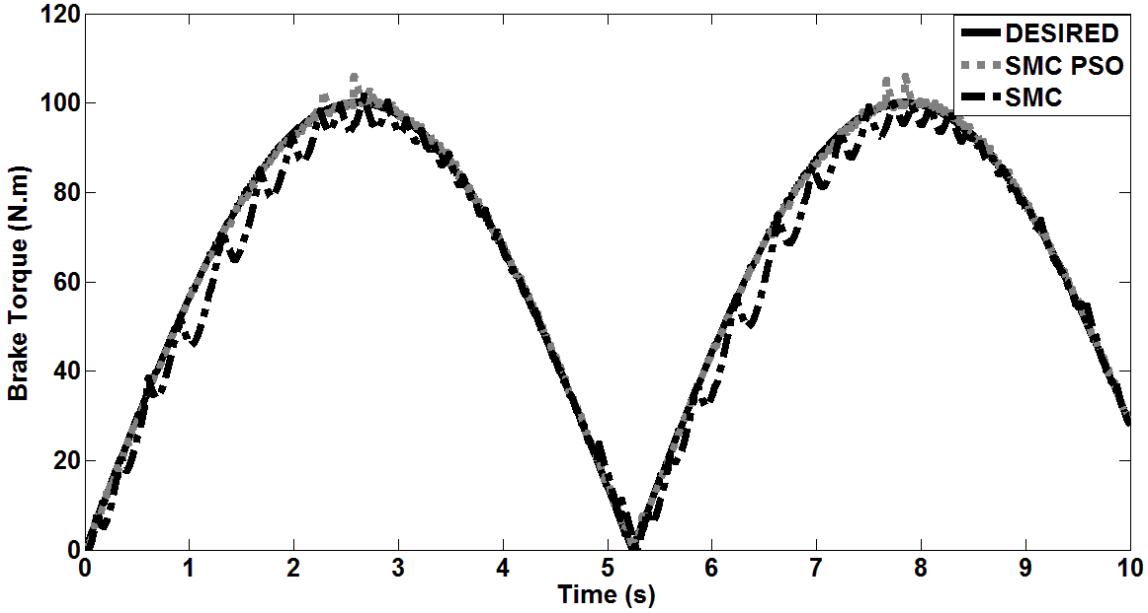

Figure 13. Graph of SMC optimized by PSO for 100 Nm at 0.5 Hz

6.0 CONCLUSION

In this study, two types of controller have been developed for an automatic braking system. The brake model presented manages to achieve an acceptable brake torque for the vehicle. To achieve this, a brake system model was developed considering brake pedal, valve, air flow dynamics and brake system hydraulics. This model was shown to provide relationship between the outputs braking torque and applied pedal force. Then, the development of SMC and PID controller to control the pedal force for an automatic braking has been demonstrated. Results show that both controllers are applicable in an automatic braking system. The results obtained were evaluated and it was shown that the output of the brake torque using both controllers followed the desired brake torque. However, SMC controller is proposed to be the best controller in this application since it has the better performance and lower percentage error compared to the PID controller. Then, SMC controller was undergoing an optimization process by chosen PSO as an optimization method, where the brake torque has a better performance compared to only using SMC controller.

ACKNOWLEDGEMENT

This work is supported by Universiti Pertahanan Nasional Malaysia through a scholarship and financial support under Long term Research Grant Scheme (L.R.G.S.) with project number LRGS/B-U/2013/UPNM/DEFENSE & SECURITY-P1 entitled "Robust Stabilization of Armored Vehicle Firing Dynamics using Active Front Wheel Steering System", led by Associate Professor Dr. Khisbullah Hudha. This financial support is gratefully acknowledged.

REFERENCES

Aparow, V. R., Ahmad, F., Hassan, M. Z., & Hudha, K. (2012). Development of Antilock Braking System Based on Various Intelligent Control System. *Applied Mechanics and Materials*, 229-231, 2394–2398.

Choi, S.B., & Hedrick, J. K. (1996). Robust Throttle Control of Automotive Engines: Theory and Experiment. *Journal of Dynamic Systems, Measurement, and Control*, 118(1), 92.

Fisher, D. (1970). Brake System Component Dynamic Performance Measurement and Analysis. SAE Technical Paper 700373, doi:10.4271/700373.

Fortina, A., & Torino, P. (2003). Mauro Velardocchia and Aldo Sorniotti. *Braking System Components Modelling*, (724).

Gerdes, J. C., Maciuca, D. B., Devlin, P. E., & Hedrick, J. K. (1993). Brake system modeling for IVHS longitudinal control. *Advances in Robust and Nonlinear Control*, 119-126.

Gerdes, J. C., & Hedrick, J. K. (1997). Vehicle speed and spacing control via coordinated throttle and brake actuation. *Control Engineering Practice*, 5(11), 1607-1614.

Guo, Yuzheng, & Peng-Yung Woo. (2003). An adaptive fuzzy sliding mode controller for robotic manipulators. *Systems, Man and Cybernetics, Part A: Systems and Humans,* IEEE Transactions 33(2): 149-159.

Khan, Y., Kulkarni , P., K. Y.-T. (1994). Modeling, Experimentation and Simulation of a Brake Apply System. *Journal of Dynamic Systems, Measurement, and Control*, 116(1994), 111–122.

Liang, H., Chong, K. T., No, T. S., & Yi, S. (2002). Vehicle longitudinal brake control using variable parameter sliding control, 11, 403–411.

Maciuca, D. B., Gerdes, J. C., & Hedrick, J. K. (1994). Automatic braking control for IVHS Dragos B. Maciuca, J. Christian Gerdes, J. Karl Hedrick (The University of California, Berkeley/U.S.A.), *JSAE Review*, 16(2), 219.

Maciuca, D. B., & Hedrick, J. K. (1995). *Advanced nonlinear brake system control for vehicle platooning*. In Proc. of European Control Conference, 5-8.

Milanés, V., González, C., Naranjo, J. E., Onieva, E., & De Pedro, T. (2010). Electro-hydraulic braking system for autonomous vehicles. *International Journal of Automotive Technology*, 11(1), 89–95.

Shaomin, L. O. U., Zhen, F. U., Lechao, Z., & Cangsu, X. U. (2010). *Integrated Control of Semi-active Suspension and ABS Based on Sliding Mode Theory*. In Proceedings of the 29th Chinese Control Conference, 3214–3218.

The University of Michigan. (1996). Design Model of a Vacuum-Assisted Hydraulic Braking System. Ann Arbor, MI 48109-2125: Krishnamachari, R. S.

Yamada, T. & Sawada, M., (2001). Development and Implementation of Simulation Tool for Vehicle Brake System. SAE Technical Paper 2001-01-0034, 2001, doi:10.4271/2001-01-0034

Yan, Z. P., Deng, C., Zhou, J. J., & Chi, D. N. (2012). *A novel two-subpopulation particle swarm optimization*. In Proceedings of the World Congress on Intelligent Control and Automation *(WCICA)*, 4113–4117.